SSRG International Journal of Mechanical Engineering
ISSN: 2348-8360/ https://doi.org/10.14445/23488360/IJME-V11I11P104

Volume 11 Issue 11, 34-46, November 2024

Original Article

Influence of Operating Parameters and Rib Convexity on Friction Torque of Taper Roller Bearings

Amisha B. Khant[1], Jaydeep K. Dadhaniya[2]

[1,2]*Department of Mechanical Engineering, Gujarat Technological University, Ahmedabad, India.*

[1]*Corresponding Author : amisha.khant@gmail.com*

Received: 11 September 2024 Revised: 15 October 2024 Accepted: 10 November 2024 Published: 30 November 2024

Abstract *- In the context of minimizing the bearing power loss and improving the performance of Tapered Roller Bearings (TRBs), accurate estimation of friction torque is necessary. At high axial load, the Friction Torque (FT) in TRBs increases rapidly, leading to significant power loss and heat generation within the bearings, which raises the bearing Temperature (BT). This paper investigates the effect of three parameters, inner raceway rib convexity, pure axial load and Bearing rotating speed on FT and BT of TRBs. Experiments are conducted on friction torque test rig using L27 full factorial DOE with rib convexity (0,3,6 µ), axial load (2000, 4000, 6000 kgf), speed (400, 500, 600 rpm). Based on the experimental work, a regression model with an accuracy of 98.87% and 99.36% for FT and BT, respectively, is developed using Minitab19. Analysis of Variance (ANOVA) and regression analysis is used to check the model adequacy. The Desirability Function Approach (DFA) is adopted to optimize multiple responses simultaneously. Conformation experimentation has been done to validate the work.*

Keywords *- Analysis of Variance, Friction Torque, L27 Full Factorial Design, Rib Convexity, Tapered Roller Bearings*.

1. Introduction

The history of rolling bearings spans more than 5,000 years. Between A.D. 44 and 54, the Romans created three different varieties of rolling bearings, now known as ball bearings, cylindrical roller bearings, and tapered roller bearings (TRBs)[1]. TRBs are essential components in various mechanical machinery, offering smooth rotational motion combined with high radial and axial load-carrying capacities. The development of early TRBs marked a significant advancement in bearing technology. H. Timken first invented the TRB, which became a famous invention due to its primary purpose of reducing friction in wagon wheels and transferring loads smoothly. Initially, TRBs were not employed for high-speed applications, as the increased friction torque led to high heat generation. However, advances in bearing design, improvements in manufacturing accuracy, and the identification of effective lubrication methods for heat removal have gradually increased the acceptable operating speeds for TRBs [2, 3, 4]. Modern machinery operates at high power density and speed to meet the demands of daily services. TRBs are widely used in heavy-duty machinery and automobiles because of their ability to accommodate high loads. However, they also result in significant frictional torque, leading to energy loss, heat generation, increased bearing temperature, decreased performance, and ultimately reduced bearing life [5]. The generation of frictional torque in TRBs is inevitable and influenced by several factors, including rolling and sliding friction between rollers, raceways, the cage, roller skewing, proper lubrication selection, load conditions, operating conditions, misalignment, bearing temperature, contamination, manufacturing tolerances, geometric irregularities, and surface defects. As a result, studying frictional torque in TRBs becomes a complex endeavor.

2. Literature Review

In the last few decades, many researchers have developed empirical equations for the prediction of friction torque accurately[6]. The friction torque produced in TRBs is merely divided into two ways: a) load-dependent friction torque that varies with the applied load and b) load-independent one that regardless of the load. FT through load dependency considered a) rolling friction involving rollers and raceways, b) sliding friction occurring between the rollers ends and rib, while FT through load independent factors involve a) sliding friction between rollers and roller cage, and (b) drag friction caused by the viscosity of the considered lubricant [7, 8]. An accurate estimation of the FT for any rolling bearing at moderate applied load and speed is necessary to study load dependents and independent components properly. At a limited speed, the effect of load-independent components is comparatively small compared to the former. Hence, in most research, only load-dependent components have been included in the analysis [7, 8]. Figure 1 shows the friction toque composition with dependent load, and Figure 2 shows the dependent and independent load components.

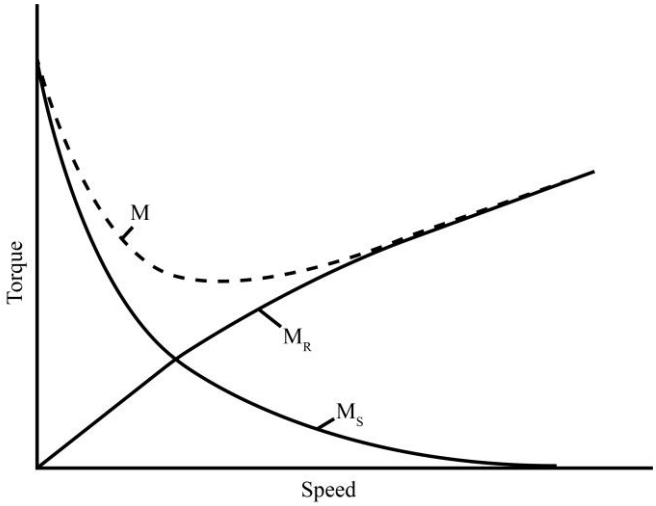

Fig. 1 TRBs torque composition with load-dependent components [7]

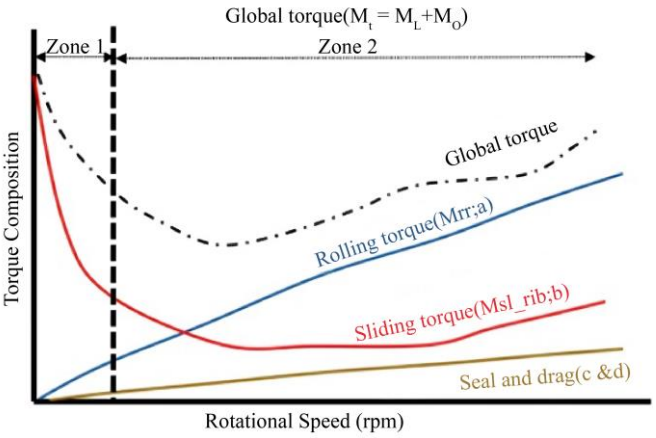

Fig. 2 TRBs torque with load-dependent and independent components [8]

P. L. Wu et al. [6] presented a review examining the theoretical models for analyzing friction torque in rolling bearings(RBs) with an outline of various measurement techniques for assessment. Z. H. Wu et al. [9 indicated that normally, compared to oil lubrication, grease in RBs has many advantages, such as a large operating temperature span, high excessive pressure and adhesion properties, and the establishment of the lubricating device becomes relatively simple. Witte [10][5] developed an operating torque predicting method that established a dimensional analysis of the EHD variables associated with the operating conditions in TRBs for pure thrust and combined thrust and radial loads—explained the measurement of the torque origins in a TRBs, considering the torque characteristics of the interaction between the ribs and rollers. Karna [11] carried out experimental work to establish the analytical expression to predict the frictional torque on TRB with detached rib with axially applied load. Jamison et.al. [12] presented that skewing of rollers in TRBs occurs due to several kinds of inconsistencies in manufacturing and the frictional force between the roller end and rib, resulting in a one-sided torque about the center of pressure in the roller pathway. S. Aihara [7] introduced a novel torque calculation formula for TRBs subjected to axial loads to address discrepancies observed in conventional formulas as the methods for estimating the running torque of TRBs at that time frequently demonstrated deviations from actual values, especially when axial loads were applied. Zhou et al. [13] proposed a torque model using both theoretical analysis and experimental validation that involves EHL lubrication and can predict torque for each roller. A bearing torque experiment test rig has been constructed to measure the torque of the cone race, rib and cup race separately. Wang et al. [14] presented a dynamic model for the frictional torque within a TRB and the corresponding heat generation rates at the contact points that are influenced by the forces and internal speeds.

Paleu et al. [15] created a test setup to observe the changes in both friction torque and bearing temperature in highspeed rolling bearings, with the capability to run at speed till 120,000 rpm. An advanced data gaining methods and a virtual instrument were utilized to track the friction torque in bearing. Tiago Cousseau [16] identified a method for friction behaviour in rolling bearings with two different types of grasses. Lugt [17] describes a review of grease lubrication that includes grease flow, fluid film formation and reduction with dynamic performance of the grease life. This study also reviewed the effect of grease on friction torque compared to previous studies.

Y. Liu et al. [18] proposed models and analyses of how varying axial loads, rotating speeds, and cage slip rates influence the geometric homogeneity of the tapered rollers. L Liu. et al. [19] presented the influence of raceway convexity on the FT of TRBs using experimental work and theoritical model. Seungpyo Lee et al. [20] considered roller geometries with combine effect of material uncertainty on FT in TRBs with operating parameter axial load using Monte Carlo simulation. P Wingertszahn et al. [21] presented a research that introduces a simulation model of parametric multibody to predict the friction torque with kinematics of TRBs.

Manjunath et al. [8] examined the friction torque due to rolling resistance and thermal inlet shear factor within TRBs through number of organized experiments employing a modular test setup. The research involves testing measurements of the overall frictional torque when subjected to axial load at varying speeds and oil temperatures. M. Wrzochal [22] introdused a new device that measure the FT during the production along with applied axial load and other bearing parameters. S. Wirsching et al. [23] A proposed numerical optimization method that uses large radius spherical forms on the roller's end face paired with tapered rib geometry helps to successfully reduce friction by improving the macro-geometric parameters in EHL of roller face and rib contact. Guohua Cai et al. [24] has proposed a method to measure the

FT in TRBs between rollers and raceways at heavy redial load conditions. XinBin Li [25] identified enhanced method to calculate FT in TRBs with both type of loading conditions.

Previous studies have extensively investigated friction torque in TRBs through various approaches. However, none have specifically addressed the influence of key operating parameters such as pure axial load speed and geometrical parameter rib convexity on friction torque in TRBs. These factors are particularly critical when TRBs are used in the wheel hubs of heavy-duty vehicles, especially during turns [26]. In turning conditions, the wheel hub experiences a high axial load, causing friction torque to increase rapidly between the larger face of the roller and the rib, leading to a rise in bearing temperature. To reduce power loss and extend bearing life, it is essential to minimize friction torque and control bearing temperature by accurately estimating the combined effects of load, speed, and rib convexity. Additionally, the impact of these parameters on friction torque has not yet been statistically optimized using full factorial DOE and DFA. Therefore, the primary objective of this study is to evaluate the effects of rib convexity, axial load, and speed on friction torque (FT) and bearing temperature (BT) in TRBs and develop an analytical model that can accurately predict friction torque and bearing temperature within a specified range of these parameters.

3. Material and Methods

3.1. Experimental Setup

TRB has versatile applications based on its specifications and loading conditions. Here, a particular application for the TRB bearing is considered to select the bearing size and specifications and confirm the features and technical specifications of the test rig. The selected TRB has an inner diameter of 90 mm and an outer diameter of 150 mm assembled inside the vehicle's front wheel hub, with a maximum loading capacity of 6 tons and a wheel diameter of 1008 mm. Experimental test rigs must be prepared and calibrated carefully for accurate and consistent outcomes. Preparatory steps for the test rig are as follows.

3.1.1. FT Test Rig Assembly

The assembly of the test rig is shown in Figure 3 for measuring a friction torque for TRBs that are controlled with the Supervisory Control and Data Acquisition (SCADA) system, as shown in Figure 4. The main units of the test rig are (1) a drive unit that is driven by an AC induction motor comprising a pulley and two supported ball bearings and (2) a Test bearing unit, known as a bearing hub, consisting of a TRB test bearing along with one support bearing. The test bearing is assembled inside the test housing with the assistance of a bearing holder (3) Coupling unit connects the drive unit to the test bearing unit with two backless couplings through a torque sensor (4) hydraulic load unit consists of hydraulic cylinder set by the adjusting hydraulic flow control valve to vary an axial load on the test bearing. A thrust ball bearing supports the test bearing holder, which has a high dynamic axial load-carrying capacity higher than the test bearings. (5) The control unit is based on the SCADA system attached to the test rig, which collects the data of FT, BT, Axial load, and rpm through sensors and records on the system. Torque sensors, temperature sensors, load sensors and speed sensors are accurately calibrated to ensure high accuracy and reliability.

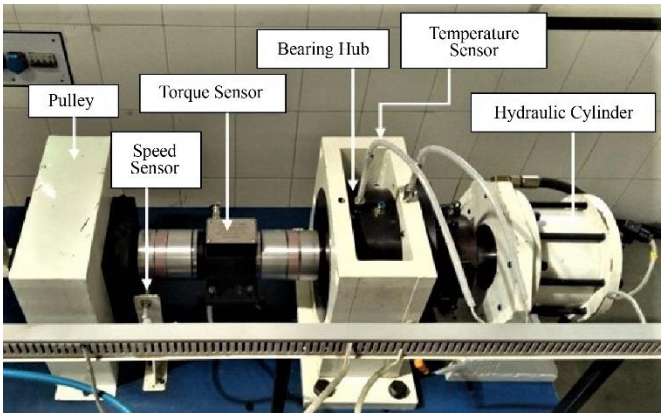

Fig. 3 Friction torque test rig

3.1.2. Test Rig Features and Technical Specifications

This test rig accommodates the test TRB bearing with an inner diameter of up to 135 mm and an outer diameter of up to 200 mm; however, as per the bearing application consideration, the bearing hub is prepared as it accommodates a bearing with an inner diameter of 90 mm and outer diameter of 150 mm. The features and technical specifications of the test rig are shown in Table 1. The hydraulic cylinder applies the axial load on the test bearing up to 10000 kgf and can be applied continuously up to 1200 bearing rpm. Friction torque on the bearing measured with a torque sensor has the capacity to measure torque up to 500 Nm. The rotational speed of the shaft can be maximized up to 1200 rpm.

Fig. 4 Data logging on SCADA

Table 1. Test rig specifications

Bearing size	90 mm ID and 150 mm OD
Axial Load	10,000 kgf Max
Rpm	1200 Max
Running Torque	500 Nm Max
Lubrication	Grease (High Lub LT 2 EP)

3.2. Experiment Preparation

The arrangements of the main components of single-row TRB are shown in Figure 5(a). The cross sectional view is as shown in Figure 5(b). Table 2 shows the dimensional specification of tested TRBs. Convexity of the outer raceway, inner raceway and rollers are considered as 6µ, 6µ and 4µ (maximum), respectively, and surface roughness (Ra) for raceways, roller surfaces and rib is considered as 0.2 µm (maximum) for tested bearings.

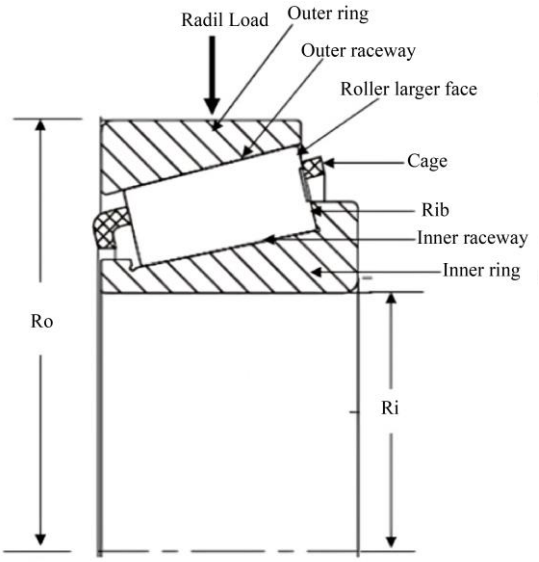

Fig. 5(a) Tapered roller bearing

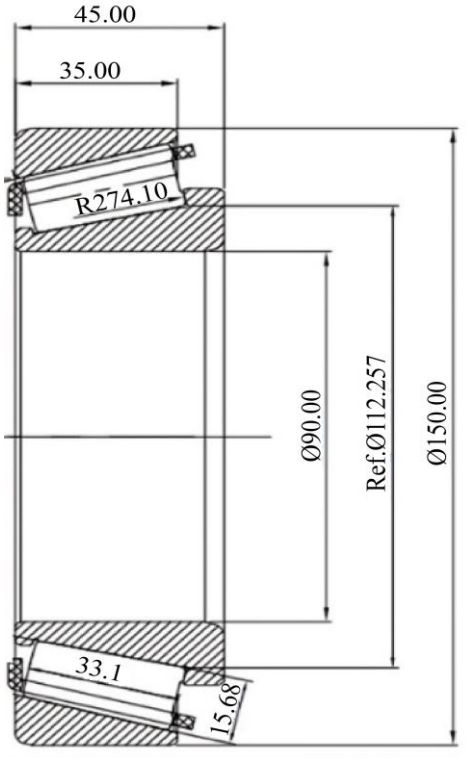

Fig. 5 (b) TRB cross-sectional view

Table 2. Specification of the sample TRBs

Nominal outside diameter, mm	150
Nominal bore diameter, mm	90
Nominal width, inner ring, mm	45
Nominal width, outer ring, mm	35
Number of rollers	23
Material	SAE52100

Three TRBs were manufactured and assembled separately with careful attention to the required specifications, maintaining approximate identical characteristics except for the rib convexity of the inner raceways. Many inner raceways were produced with required specific rib convexities and were measured using a TALYSURF surface roughness tester. Three inner raceways with rib convexities of approximately 0µm, 3µm, and 6µm, as shown in Figures 6 (a), (b) and (c), respectively, were selected for further assembly and the intended research purposes.

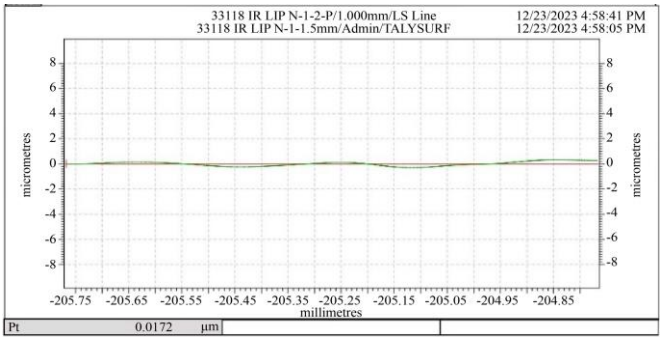

(a) 0 µm (Approx)

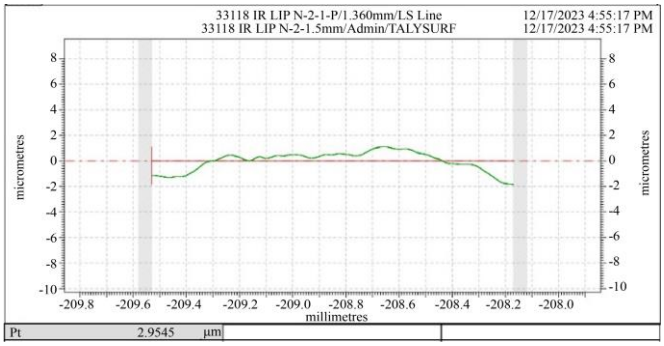

(b) 3 µm (Approx)

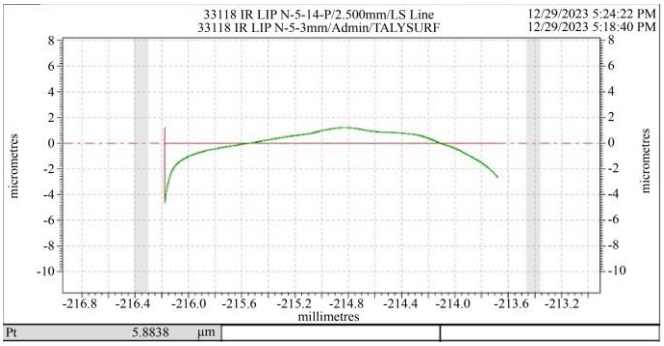

(c) 6 µm (Approx)

Fig. 6 Rib convexity profiles

3.3. Design of Experiments

Mechanical experiments always involve lots of physical effort and different kinds of costs like material costs, experimental design running costs, etc. It is also time consuming if not planned properly. Design of Experiments (DOE) is the set of methods that analyze the possibilities of experimental work with the minimum number of experiments [27], saving lots of human efforts and overall cost.

Full factorial designs, Fractional factorial, Taguchi Designs, and Response surfaces are popular types of DOE often preferred by researchers. Full factorial design is the most widely used method that allows all the possible interaction effects between all the factors and offers higher precision in estimating factor effects [28]. In order to create a statistical model for the Friction Torque (FT) in Nm and Bearing Temperature (BT) in °C, L27 full factorial DOE with all possible interactions has been considered for the experimentation. Each experiment is replicated three times, and the average of all three readings is considered to be the response of the experiments. Minitab19 analytical software is used to analyze the interaction effects. Randomization is used for experiment runs, ensuring mutual exclusivity of runs.

Several pilot experiments were conducted before the final experiments to define the appropriate levels of each factor for the desired objectives. During the pilot phase, the axial load was varied from 1000 kgf to 8,000 kgf, the rib convexity was varied from 0 to 9 µm, and the bearing speed was tested within the range of 100 rpm to 800 rpm according to the bearing specifications and considered application. These pilot experiments involved different combinations of axial load, rib convexity, and bearing speed. From the results and observations of the pilot experiments, it was concluded that when the axial load exceeds 6000 kgf with the bearing speed exceeds 600 rpm, the bearing temperature increases rapidly above 120°C, which is higher than the permissible temperature range for sealed beatings according to the bearing standards. Also, discolouration was observed on the contact surface of the raceway and rib due to heat generated during the test.

Furthermore, it was found that when the rib convexity exceeds 6 µm, the contact stress increases higher than 4000 MPa, beyond the permissible range of the bearings as per the standards. Based on these findings, the present study considers three factors—Rib Convexity (A), Axial Load (B), and Operating Speed (C)—each at three levels. Table 4 shows all possible combinations along with the responses that were obtained.

FT was measured continuously using SCADA, and the maximum obtained value was considered for analysis. Here, Hertzian contact stress at the roller end and inner raceway rib becomes essential to be included in the study as at high axial load, and the contact stress rises and enhances bearing temperature. Hertzian contact stress theory has been classified as point contact for TRBs [11] and calculated at different convexities and loads with the help of MESYS AG contact stress calculation software. Results ensured that it does not exceed more than 2400 MPa at any load and convexity combinations considered here and, hence, is safe per bearing standards [29].

Table 3. Factors and their selected levels

Factors	Level			Unit
	1	2	3	
Rib Convexity (A)	0	3	6	µ
Axial Load (B)	2000	4000	6000	kgf
Speed (C)	400	500	600	rpm

3.4. Interaction Effects between Parameters

Experimental results, as shown in Table 4, in accordance with main effect plots for FT and BT shown in Figures 7 and 8, respectively generated using MINITAB 19, indicate the interaction effect of an independent variable on responses. Figure 7 shows that the axial load and speed increase as FT increases and rib convexity decreases. Friction torque is maximum when rib convexity is 0 µ, an axial load is 6000 kgf, and speed is 600 rpm and vice-versa. It is minimum when rib convexity is 6 µ, an axial load is 2000 kgf, and rpm is 400 rpm. But as compared to FT plot effects with BT plot effects, it indicated that when the friction torque is minimum at rib convexity 6 µ but, Figure 8 shows that at some convexity, BT is maximum. It happens due to contact stress because as the rib convexity decreases, the contact stress between the rib and roller tip increases. Hence, the BT increases rapidly due to friction increases. Figure 8 shows that BT increases as the load and speed increase as the friction increases simultaneously.

Figures 9 and 10 show interaction plots for FT and BT based on the analysis of experimental results, as shown in Table 4 using MINITAB 19. It is a detailed graphical presentation of dependent variables over independent variables' interaction effects. In Figure 9, the Y-axis presents the FT, the response with three different interaction plots of A*B, A*C and B*C, respectively. Here, the top left plot and bottom left plot show lines are not parallel, which means that convexity has a good impact on FT while axial load is applied and speed is increased, respectively.

On the other hand, the bottom left plot shows that the lines are parallel and closer, showing weaker interaction between axial load and bearing speed. It shows that there is little impact of axial load and bearing speed varying alone on friction torque. Figure 10, Y-axis presents the BT, the response of three different interaction plots, the same as A*B, A*C, and B*C. As compared to Figure 9 and Figure 10, convexity has a higher impact on FT and BT. Furthermore, Figure 9 shows that as the rib convexity increases, it decreases the FT, while Figure 10 shows that as the convexity increases to the third level, the BT goes high.

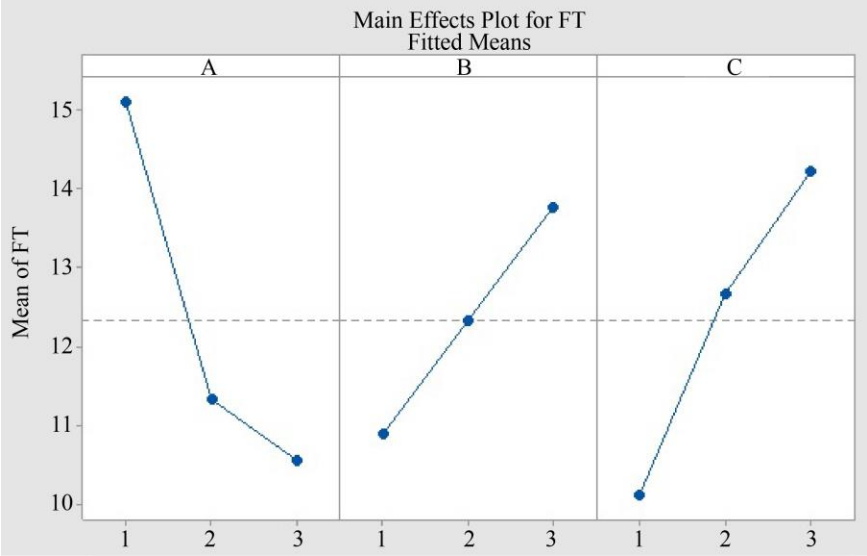

Fig. 7 Main effective plots for FT

Table 4. L27 Full factorial DOE with experimental results FT and BT

Std. Order	Run Order	A	B	C	FT	BT
1	26	1	1	1	12	65
2	25	1	1	2	14	72
3	8	1	1	3	15	79
4	14	1	2	1	13	74
5	6	1	2	2	15	80
6	20	1	2	3	16	87
7	23	1	3	1	15	79
8	18	1	3	2	17	86
9	1	1	3	3	19	96
10	19	2	1	1	8	55
11	24	2	1	2	10	61
12	12	2	1	3	11	65
13	22	2	2	1	9	61
14	3	2	2	2	12	67
15	13	2	2	3	14	73
16	7	2	3	1	10	64
17	16	2	3	2	13	72
18	21	2	3	3	15	79
19	5	3	1	1	7	67
20	2	3	1	2	10	73
21	4	3	1	3	11	81
22	11	3	2	1	8	74
23	10	3	2	2	11	79
24	9	3	2	3	13	87
25	27	3	3	1	9	78
26	15	3	3	2	12	85
27	17	3	3	3	14	93

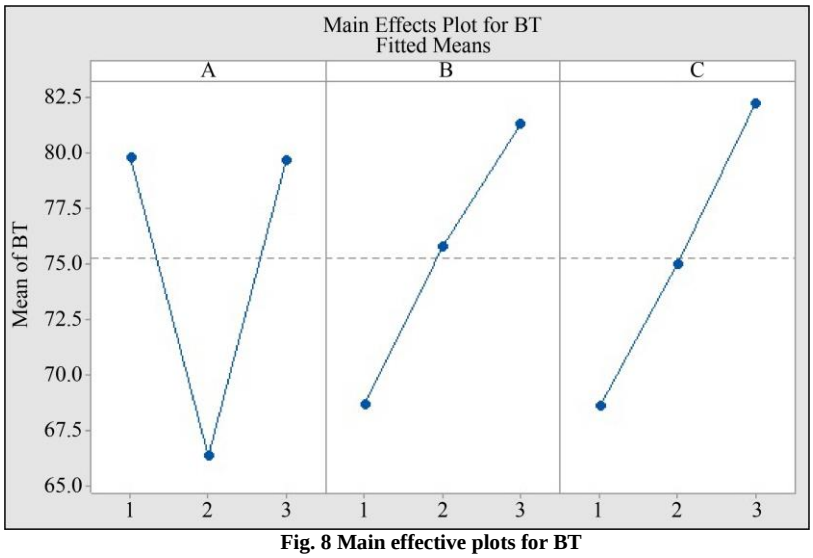

Fig. 8 Main effective plots for BT

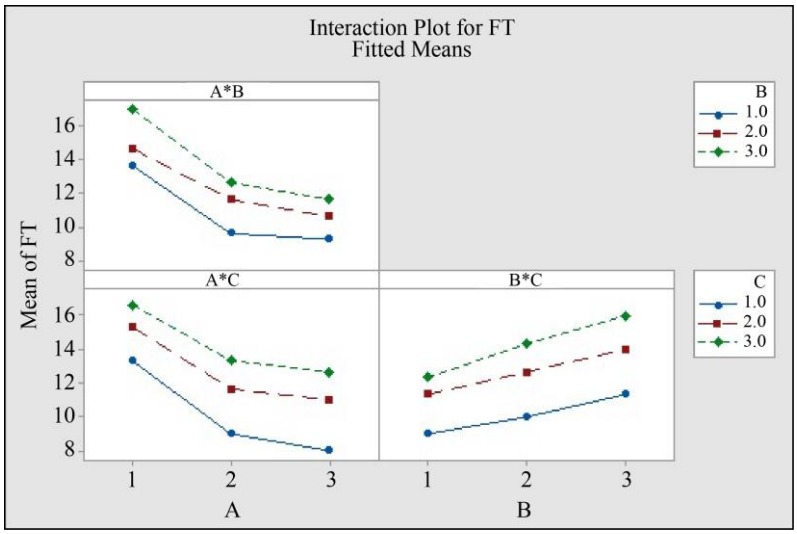

Fig. 9 Interaction plots for FT

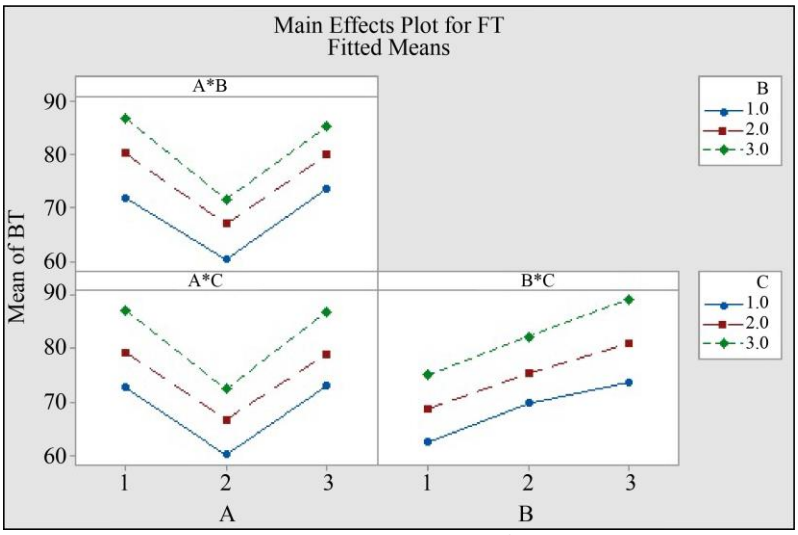

Fig. 10 Interaction plots for BT

4. Development of Regression Model for FT and BT

4.1. Regression modeling for FT and BT

TRBs operate under complex conditions where many factors simultaneously affect the performance of the bearing. Predictive models are used to establish the relationship between the responses and the system's controlled factors. Predictive models can be further classified into various categories, such as statistical models, machine learning models, Neural Networks, soft computing models, etc, based on their working basis and application. A mathematical model that represents the relation between responses and independent variables is called Regression Model. This model can be used for predicting the parameter, process optimization or process control. The second-order regression model, also called the quadratic model, can offer higher predictability than the first-order model and is more reliable when there is more than one predictor. Hence, a second-order multiple regression model is selected for the presented work. The generalized quadratic regression equation can be presented by Equation (1)

$$y = \beta_0 + \beta_1 x_1 + \beta_2 x_2 + \ldots + \beta_{12} x_1 x_2 + \beta_{13} x_1 x_3 + \ldots + \beta_{11} {x_1}^2 + \beta_{22} {x_2}^2 + \ldots \quad (1)$$

Where y represents response, x_1, x_2, x_3... represents controlled factors, also called independent variables and β_0, β_1, β_2 … are the partial regression coefficients [29]. As shown in Table 4, the full factorial DOE was analyzed using Minitab 19. The normal probability plots of residual vs fit from the analyzed full factorial design for FT and BT are shown in Figures 12 and 13. As shown in the figures, both the plots for FT and BT present a linear relationship as the p-value presented more than 0.05. Hence, in this present work, multiple linear regression analysis is applied to establish the relationship between independent variables rib convexity, load and speed with dependent variables FT and BT, respectively. Regression analysis is carried out using Minitab 19 with a 95% confidence level. These developed regression models for FT and BT are shown in Equations (2) and (3), respectively.

$$FT = 14.89 - 8.444\,A + 1.278\,B + 2.722\,C + 1.500\,A*A - 0.500\,C*C - 0.250\,A*B + 0.333\,A*C + 0.333\,B*C$$
$$R^2 = 98.87\%,\ R^2(\text{adj}) = 98.27\% \quad (2)$$

$$BT = 91.37 - 51.61\,A + 9.61\,B + 4.11\,C + 13.389\,A*A - 0.778\,B*B + 0.389\,C*C - 0.833\,A*B - 0.167\,A*C + 0.750\,B*C$$
$$R^2 = 99.36\%,\ R^2(\text{adj}) = 95.15\% \quad (3)$$

Here, R^2 shows the variation measures in the regression model, and R^2(adj) shows the variation measures for the multiple regression model. Both are used to check the integrity of the model. R^2 value can change or may remain the same as the predictor added in the model, while R^2(adj) can adjust the value only if the new predictor improves the model. So, for multiple regression analysis, R^2(adj) is considered more reliable for the model's goodness of fit. Here, as shown in Equation (2), the FT model shows R^2 = 98.87% and R^2(adj) = 98.27% and in Equation (3), the BT model shows R^2 = 99.36% and R^2(adj) = 95.15%. Both R^2 and R^2(adj) values are higher than 95%, and hence, it represents that both models adequately fit the experimental results.

4.2. Analysis of Variance (ANOVA)

Analysis of Variance (ANOVA) is a powerful statistical tool commonly used in mechanical experiments where multiple factors are being tested simultaneously to observe whether they significantly influence the response variable. Here, ANOVA is used to check the impact of multiple independent variables (load, speed and rib convexity) on response variables (FT and BT) and the adequacy of the analytical model. Up to 2-way interaction terms have been included in the model to ensure higher predictability of the model. ANOVA results for both the subsequent responses are presented in Tables 5 and 6. In these tables, DF is presented as the Degree of Freedom, and Adj SS and Adj MS are presented as the adjacent sum of squares and the adjacent mean sum of squares, respectively. F value shows the error mean square to the model mean square. The higher the F value shows, the lesser noise is presented by the P value. In Table 5 and Table 6, the regression term summarized the model's overall fit to the data. Here, the P value of the regression model for both the responses FT and BT is 0, which is less than the significance level (α = 0.05), hence representing that the model significantly explains the variability in data. Here, the terms with a P value lesser than 0.05 are significant for the model and vice versa. Insignificant terms can be omitted from the model summary by deselecting them. Table 5 shows that terms B and B*B have P values of 0.093 and 1.000, respectively, higher than 0.05; thus, these factor and interaction terms are insignificant.

Table 5. ANOVA table for FT

Source	DF	Adj SS	Adj MS	F-Value	P-Value
Regression	9	225.417	25.0463	164.82	0.000
A	1	21.042	21.0419	138.47	0.000
B	1	0.482	0.4818	3.17	0.093
C	1	2.187	2.1867	14.39	0.001
A*A	1	13.500	13.5000	88.84	0.000
B*B	1	0.000	0.0000	0.00	1.000
C*C	1	1.500	1.5000	9.87	0.006
A*B	1	0.750	0.7500	4.94	0.040
A*C	1	1.333	1.3333	8.77	0.009
B*C	1	1.333	1.3333	8.77	0.009
Error	17	2.583	0.1520		
Total	26	228.000			

Table 6. ANOVA table for BT

Source	DF	Adj SS	Adj MS	F-Value	P-Value
Regression	9	2658.08	295.34	293.58	0.000
A	1	786.01	786.01	781.33	0.000
B	1	27.26	27.26	27.10	0.000
C	1	4.99	4.99	4.96	0.040
A*A	1	1075.57	1075.57	1069.17	0.000
B*B	1	3.63	3.63	3.61	0.075
C*C	1	0.91	0.91	0.90	0.356
A*B	1	8.33	8.33	8.28	0.010
A*C	1	0.33	0.33	0.33	0.572
B*C	1	6.75	6.75	6.71	0.019
Error	17	17.10	1.01		
Total	26	2675.19			

Table 6 shows that interaction terms B*B, C*C, and A*C have P values of 0.075, 0.356, and 0.572, which are higher than 0.05; hence, these interaction terms are insignificant. Pareto charts of the standardised effect for both the responses FT and BT are shown in Figures 11 and 12, respectively. It represents that the factors (also called predictors) on the left side of the red line are insignificant. Here, for the response FT, terms B and B*B and for the response BT, terms B*B, C*C and A*C are insignificant. Insignificant terms can be omitted for the analysis in Minitab19 by deselecting them. Figures 13 and 14 show the normal probability plots for residuals of FT and

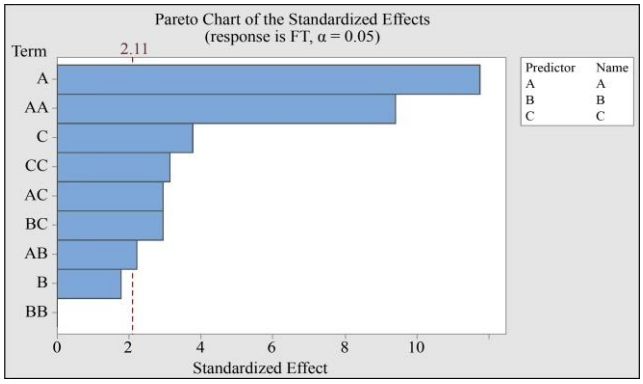

Fig. 11 Pareto chart of the standardized effect for FT

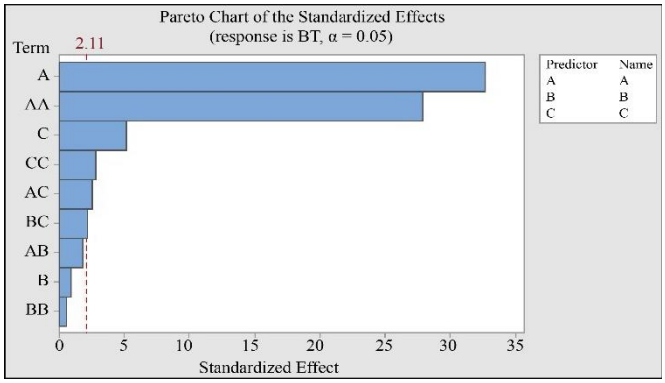

Fig. 12 Pareto chart of the standardized effect for BT

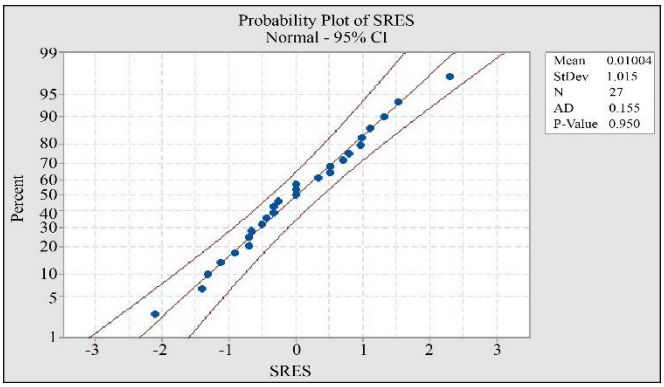

Fig. 13 Normal probability plot for residuals for friction torque

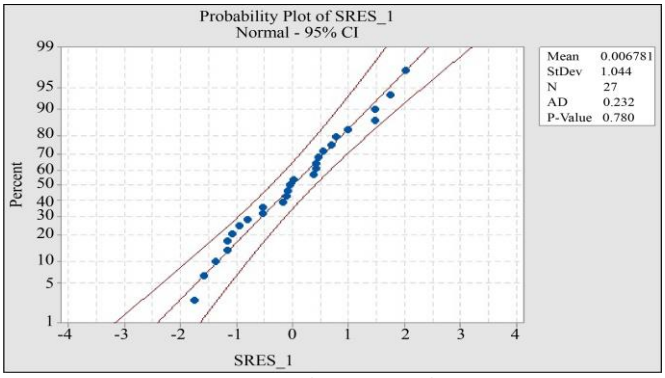

Fig. 14 Normal probability plot for residuals for bearing temperature

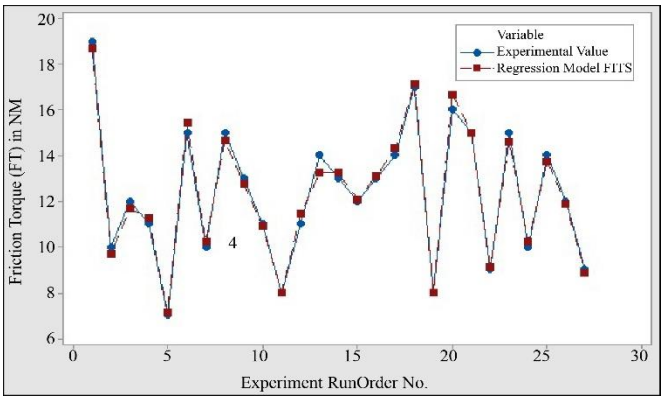

Fig. 15 FT experiment results vs. regression model fits

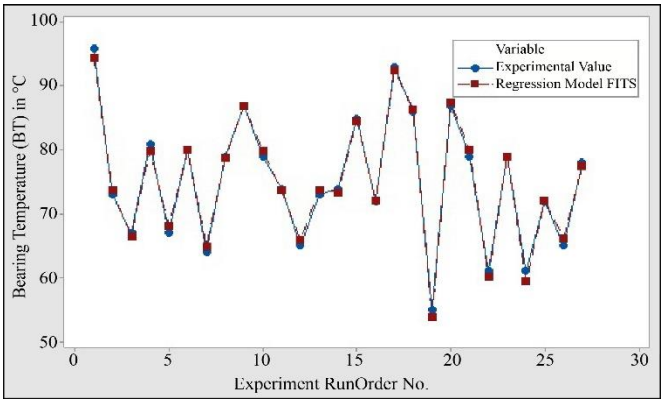

Fig. 16 BT experiment results vs. regression model fits

BT for the tested bearings. Anderson-Darling (AD) test statistics and P value for both the plots are greater than 0.05 and suggest that residuals appear normally distributed and, thus, the model to be considered valid. Table 7 compares experimental results with regression model fits with percentage errors for FT and BT. Maximum percentage error for FT and BT shows 5.56% and 2.49%, respectively. The minimum error for FT and BT are 0% and 0.02%, respectively. Figures 15 and 16 show the graphical comparison of experiment results with predicted values for FT and BT, respectively, from the regression model. Here, blue lines represent the experiment results, and red lines represent the predicted values of the regression model. These graphs represent that the experimental results are highly correlated with the developed regression model.

Table 7. Comparison of experimental results with regression model fits along percentage errors

Sr. No	Factors			Experiment		Regression		Percentage Error	
	A	B	C	FT	BT	FT_FITS	BT_FITS	FT	BT
1	1	1	1	12	65	11.8611	66.2315	1.16	1.89
2	1	1	2	14	72	13.7500	72.0926	1.79	0.13
3	1	1	3	15	79	14.6389	78.7315	2.41	0.34
4	1	2	1	13	74	13.2222	73.4259	1.71	0.78
5	1	2	2	15	80	15.4444	80.0370	2.96	0.05
6	1	2	3	16	87	16.6667	87.4259	4.17	0.49
7	1	3	1	15	79	14.5833	79.0648	2.78	0.08
8	1	3	2	17	86	17.1389	86.4259	0.82	0.50
9	1	3	3	19	96	18.6944	94.5648	1.61	1.49
10	2	1	1	8	55	8.0000	53.7870	0.00	2.21
11	2	1	2	10	61	10.2222	59.4815	2.22	2.49
12	2	1	3	11	65	11.4444	65.9537	4.04	1.47
13	2	2	1	9	61	9.1111	60.1481	1.23	1.40
14	2	2	2	12	67	11.6667	66.5926	2.78	0.61
15	2	2	3	14	73	13.2222	73.8148	5.56	1.12
16	2	3	1	10	64	10.2222	64.9537	2.22	1.49
17	2	3	2	13	72	13.1111	72.1481	0.85	0.21
18	2	3	3	15	79	15.0000	80.1204	0.00	1.42
19	3	1	1	7	67	7.1389	68.1204	1.98	1.67
20	3	1	2	10	73	9.6944	73.6481	3.06	0.89
21	3	1	3	11	81	11.2500	79.9537	2.27	1.29
22	3	2	1	8	74	8.0000	73.6481	0.00	0.48
23	3	2	2	11	79	10.8889	79.9259	1.01	1.17
24	3	2	3	13	87	12.7778	86.9815	1.71	0.02
25	3	3	1	9	78	8.8611	77.6204	1.54	0.49
26	3	3	2	12	85	12.0833	84.6481	0.69	0.41
27	3	3	3	14	93	14.3056	92.4537	2.18	0.59

5. Results and Discussions

5.1. Simultaneous Optimization for responses FT and BT

Here, experimental work involves two responses, FT and BT. The main objective of this work is to minimise the FT as it helps reduce energy loss and heat generation, hence improving bearing performance and eventually improving. However, it is also required to keep BT at the desired range because higher BT can cause serious bearing issues like reduced bearing capacity, lubrication deterioration, heat cracks, etc. and ultimately, a decline bearing life. Hence, simultaneous optimisation has been considered here using the DFA technique.

DFA is a popular technique first introduced by [27] and popularised by [30]. It is considered a useful approach to optimize multiple responses. According to DFA, first, each response is converted into an individual desirability index d_i that varies between ranges (0, 1). When the response reaches the goal or target, then d_i =1 and when it fails to reach or is not within an acceptable range, then d_i = 0. The desirability index is calculated according to desirability functions [29] Nominal-the-best Equation (4), Lager-the-better Equation (5) and Smaller-the-best Equation (6) D C Montgomery. In these equations, y is the response value, L is the minimum of the responses, U is the maximum of the responses, and T is the

targeted value for the response. Here, r, r_1 and r_2 indicated weightage for each response normally taken as 1. Then rank-based design factors are selected as given by Equation (7) to maximize (optimize) the overall desirability D. Here, a Smaller-the-better type is considered for the FT, and Nominal-the-best is considered for the BT. The targeted value for the FT is considered a minimum from the responses, and the targeted value for BT is considered 65° as it is preferable for bearing operating temperature [29].

i) Nominal-the-best: if target T is considered between the Lower L and Upper U limits for the response y.

$$di = \begin{cases} 0 & \\ \left(\frac{y-L}{T-L}\right)^{r1} & y<L \\ \left(\frac{U-y}{U-T}\right)^{r2} & L \le y \le T \\ 1 & T \le y \le U \\ & y>U \end{cases} \quad (4)$$

ii) Larger-the-better: if target T is the maximum value for the response y.

$$di = \begin{cases} 0 & \\ \left(\frac{y-L}{T-L}\right)^{r} & y<L \\ 1 & L \le y \le T \\ & y>T \end{cases} \quad (5)$$

iii) Smaller-the-better: if target T is the minimum value for the response y.

$$di = \begin{cases} 0 & \\ \left(\frac{y-L}{T-L}\right)^{r} & y<T \\ 1 & T \le y \le U \\ & y>U \end{cases} \quad (6)$$

$$D = (d1.d2.d3 \ldots . dm)^{1/m} \quad (7)$$

Where D is the overall desirability of the responses, m represents the number of responses. Table 8 shows each response's calculated desirability index, overall desirability (D), and rank using DFA.

Table 8. Optimization using DFA

Ex. No	Factors			Experiment Value		Desirability Index		Overall Desirability (D)	Rank
	A	B	C	FT (Nm)	BT (°C)	FT	BT		
1	1	1	1	12	65	0.76376	1.00000	0.38188	8
2	1	1	2	14	72	0.64550	0.87988	0.28398	15
3	1	1	3	15	79	0.57735	0.74053	0.21377	19
4	1	2	1	13	74	0.70711	0.84242	0.29784	14
5	1	2	2	15	80	0.57735	0.71842	0.20739	22
6	1	2	3	16	87	0.50000	0.53882	0.13470	24
7	1	3	1	15	79	0.57735	0.74053	0.21377	19
8	1	3	2	17	86	0.40825	0.56796	0.11593	25
9	1	3	3	19	96	0.00000	0.00000	0.00000	27
10	2	1	1	8	55	0.95743	1.15004	0.55054	1
11	2	1	2	10	61	0.86603	1.06256	0.46010	4
12	2	1	3	11	65	0.81650	1.00000	0.40825	6
13	2	2	1	9	61	0.91287	1.06256	0.48499	2
14	2	2	2	12	67	0.76376	0.96720	0.36936	10
15	2	2	3	14	73	0.64550	0.86136	0.27800	17
16	2	3	1	10	64	0.86603	1.01600	0.43994	5
17	2	3	2	13	72	0.70711	0.87988	0.31109	12
18	2	3	3	15	79	0.57735	0.74053	0.21377	19
19	3	1	1	7	67	1.00000	0.96720	0.48360	3
20	3	1	2	10	73	0.86603	0.86136	0.37298	9
21	3	1	3	11	81	0.81650	0.69561	0.28398	15
22	3	2	1	8	74	0.95743	0.84242	0.40328	7
23	3	2	2	11	79	0.81650	0.74053	0.30232	13
24	3	2	3	13	87	0.70711	0.53882	0.19050	23
25	3	3	1	9	78	0.91287	0.76200	0.34780	11
26	3	3	2	12	85	0.76376	0.59568	0.22748	18
27	3	3	3	14	93	0.64550	0.31109	0.10040	26

Table 9. Confirmation experiments

Sr. No	Factors			Initial		Predicted		Confirmation Experiments		Percentage Error (Conf. vs. Predicted)	
	A	B	C	FT	BT	FT_FITS	BT_FITS	FT	BT	FT	BT
1	2	1	1	8	55	8.0000	53.7870	8	54	0.00	0.39
2	3	2	3	13	87	12.7778	86.9815	13	85	1.71	2.33
3	3	2	2	11	79	10.8889	79.9259	11	78	1.01	2.47
4	1	3	1	15	79	14.5833	79.0648	14	81	4.17	2.39
5	2	1	3	11	65	11.4444	65.9537	11	66	4.04	0.07

Table 8 represents the highest desirability at Rank 1 obtained at factors A2, B1, and C1. Hence, at 3µ rib convexity, 2000 kgf load and 400 rpm is the best combination for the minimal generation of friction torque and, hence, bearing temperature at a selected range of parameters. Graphical presentation for the highest mean can be presented as shown in Figure 17 using Minitab19. The beauty of full factorial DOE is that it gives the optimal results through all the possible interactions. Hence, this optimal solution is the final with no need for further improvement with different level combinations of independent variables.

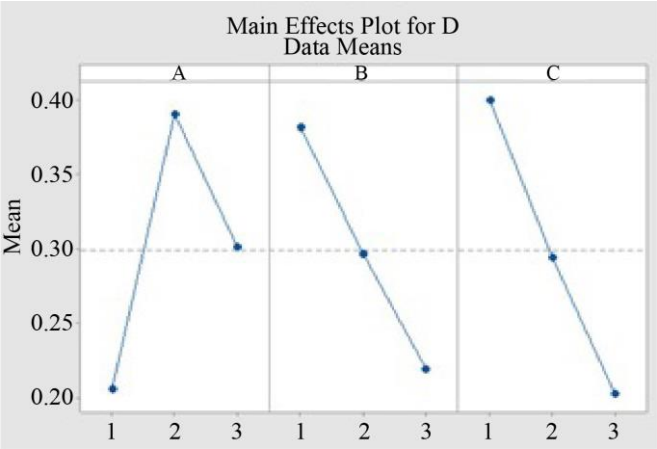

Fig. 17 Main effective plots for optimum mean obtained from DFA using Minitab19

5.2. Confirmation Experiment

Five confirmation experiments have been carried out based on the regression model. Randomly predicted factors from the model with levels are shown in Table 9. The result summary, along with the results of the initial experiments, predicted results from the regression model, and confirmation experiments, are shown in Table 9. The maximum percentage error for FT is 4.17%, and for BT, it is 2.47%. Confirmation test results show that the percentage errors are within 5%, and hence, it validates this developed regression model with good agreement with the results of the conducted experiments.

6. Conclusion

The present work proposed a statistical approach that helps minimize friction torque in TRBs under optimal operating parameters and geometrical factors. A regression model was developed based on experimental results to optimise the FT and BT of TRBs. DFA approach was adopted for the multiple simultaneous optimizations and found that the 3µ rib convexity, 2000 kgf load and 400 rpm is the best combination for the minimize the friction torque of TRBs for the selected range for the factors in the present research. FT and BT are the main responses to the regression model using full factorial DOE. The predicted values obtained from the regression model are compared with the initially conducted experiment and further conducted experiments that show the improvements and validation of the work. This designates that the developed model agrees with the experimental work and is appropriate.

Future work: The present work demonstrated the simultaneous optimization for the responses FT and BT using DFA. This methodology is further used for more responses and can check the robustness. Other optimization methods like ANN and GRA can be explored.

Acknowledgments

The authors are deeply grateful to Galaxy Bearings Ltd., Rajkot, India, for their cooperation and technical support in conducting the experiments for this research.

References

[1] Bo Jacobson, "History of Rolling Bearings," *Tribology Online*, vol. 6, no. 3, pp. 155-159, 2011. [CrossRef] [Google Scholar] [Publisher Link]

[2] R.F. Cornish, P.S. Orvos, and S.R. Gupta, "Development of High Speed Tapered Roller Bearing," 1973. [Google Scholar]

[3] Tedric A. Harris, and Michael N. Kotzalas, *Essential Concepts of Bearing Technology*, CRC Press, 5th ed., pp. 1-392, 2006. [CrossRef] [Publisher Link]

[4] Tedric A. Harris, Michael N. Kotzalas, *Advanced Concepts of Bearing Technology*, 5th ed., Rolling Bearing Analysis, CRC Press, pp. 1-368, 2006. [CrossRef] [Publisher Link]

[5] Dwight C. Witte, "Operating Torque of Tapered Roller Bearings," *ASLE Transactions*, vol. 16, no. 1, pp. 61-67, 1973. [CrossRef] [Google Scholar] [Publisher Link]
[6] P.L. Wu et al., "Theoretical Calculation Models and Measurement of Friction Torque for Rolling Bearings: State of the Art," *Journal of the Brazilian Society of Mechanical Sciences and Engineering*, vol. 44, 2022. [CrossRef] [Google Scholar] [Publisher Link]
[7] S. Aihara, "A New Running Torque Formula for Tapered Roller Bearings Under Axial Load," *Journal of Tribology ASME*, vol. 109, no. 3, pp. 471-477, 1987. [CrossRef] [Google Scholar] [Publisher Link]
[8] Manjunath Manjunath et al., "Experimental Analysis of Rolling Torque and Thermal Inlet Shear Heating in Tapered Roller Bearings," *Machines*, vol. 11, no. 8, pp. 1-22, 2023. [CrossRef] [Google Scholar] [Publisher Link]
[9] Zheng-Hai Wu, Ying-Qiang Xu, and Si-Er Deng, "Analysis of Dynamic Characteristics of Grease-Lubricated Tapered Roller Bearings," *Shock and Vibration*, vol. 2018, no. 1, pp. 1-17, 2018. [CrossRef] [Google Scholar] [Publisher Link]
[10] Dwight C. Witte, and Harold E. Hill, "Tapered Roller Bearing Torque Characteristics with Emphasis on Rib-Roller End Contact," *SAE Technical Paper*, 1987. [CrossRef] [Google Scholar] [Publisher Link]
[11] C.L. Karna, "Performance Characteristics at the Rib Roller End Contact in Tapered Roller Bearings," *ASLE Transactions*, vol. 17, no. 1, pp. 14-21, 1974. [CrossRef] [Google Scholar] [Publisher Link]
[12] W.E. Jamison, J.J. Kauzlarich, and E.V. Mochel, "Geometric Effects on the Rib-Roller Contact in Tapered Roller Bearings," *ASLE Transactions*, vol. 20, no. 1, pp. 79-88, 1977. [CrossRef] [Google Scholar] [Publisher Link]
[13] R.S. Zhou, and M.R. Hoeprich, "Torque of Tapered Roller Bearings," *Journal of Tribology ASME*, vol. 113, no. 3, pp. 590-597, 1991. [CrossRef] [Google Scholar] [Publisher Link]
[14] Shao Wang, C. Cusano, and T.F. Conry, "A Dynamic Model of the Torque and Heat Generation Rate in Tapered Roller Bearings Under Excessive Sliding Conditions," *Tribology Transactions*, vol. 36, no. 4, pp. 513-524, 1993. [CrossRef] [Google Scholar] [Publisher Link]
[15] Viorel Paleu et al., "Test Rig for Friction Torque Measurement in Rolling Bearings," *The Durham University Journal*, pp. 85-91, 2004. [Google Scholar]
[16] Tiago Cousseau et al., "Experimental Measuring Procedure for the Friction Torque in Rolling Bearings," *Lubrication Science*, vol. 22, no. 4, pp. 133-147, 2010. [CrossRef] [Google Scholar] [Publisher Link]
[17] Piet M. Lugt, "A Review on Grease Lubrication in Rolling Bearings," *Tribology Transactions*, vol. 52, no. 4, pp. 470-480, 2009. [CrossRef] [Google Scholar] [Publisher Link]
[18] Yuwei Liu et al., "An Investigation for the Friction Torque of a Tapered Roller Bearing Considering the Geometric Homogeneity of Rollers," *Lubricants*, vol. 10, no. 7, pp. 1-12, 2022. [CrossRef] [Google Scholar] [Publisher Link]
[19] Lei Liu et al., "Effects of Raceway Convexity on Friction Moment of Tapered Roller Bearings," *Journal of Physics: Conference Series: 9th International Conference on Advanced Manufacturing Technology and Materials Science*, Beijing, pp. 1-8, 2022. [CrossRef] [Google Scholar] [Publisher Link]
[20] Seungpyo Lee, and Hyun Gyu An, "Evaluation of Friction Torque in Tapered Roller," *SAE International*, pp. 1-6, 2024. [CrossRef] [Google Scholar] [Publisher Link]
[21] Patrick Wingertszahn et al., "Predicting Friction of Tapered Roller Bearings with Detailed Multi-Body Simulation Models," *Lubricants*, vol. 11, no. 9, pp. 1-22, 2023. [CrossRef] [Google Scholar] [Publisher Link]
[22] Mateusz Wrzochal et al., "New Device Proposed For Industrial Measurement of Rolling Bearing Friction Torque," *Journal of Mechanical Engineering*, vol. 68, no. 10, pp. 610-622, 2022. [CrossRef] [Google Scholar] [Publisher Link]
[23] Sven Wirsching et al., "Geometrical Optimization of the EHL Roller Face/Rib Contact for Energy Efficiency in Tapered Roller Bearings," *Lubricants*, vol. 9, no. 7, pp. 1-19, 2021. [CrossRef] [Google Scholar] [Publisher Link]
[24] Guohua Cai et al., "A Measurement Method for Friction Torque Between Rollers and Raceways of Tapered Roller Bearings Under Radial Heavy Load Conditions," *Tribology International*, vol. 200, 2024. [CrossRef] [Google Scholar] [Publisher Link]
[25] Xin Bin Li et al., "Friction Moment Calculation Method for Tapered Roller Bearings Under Combined Loads," *Science China Technological Sciences*, vol. 67, pp. 2565-2578, 2024. [CrossRef] [Google Scholar] [Publisher Link]
[26] Berthold Martin, and Harold E. Hill, "Design and Selection Factors for Automatic Transaxle Tapered Roller Bearings," *SAE Technical Paper*, 1992. [CrossRef] [Google Scholar] [Publisher Link]
[27] Sir Ronald Aylmer Fisher, and Ghiuean T. Prance, *The Design of Experiments*, Hafner Press, pp. 1-248, 1974. [Google Scholar] [Publisher Link]
[28] Douglas C. Montgomery, *Design and Analysis of Experiments*, 8th ed., John Wiley & Sons, 2012. [Google Scholar] [Publisher Link]
[29] SKF, SKF General Catalogue, Sweden, 2003. [Online]. Available: https://imparayaycia.com/skfcatalogogeneral.pdf
[30] George Derringer, and Ronald Suich, "Simultaneous Optimization of Several Response Variables," *Journal of Quality Technology*, vol. 12, no. 4, pp. 214-219, 1980. [CrossRef] [Google Scholar] [Publisher Link]